^{40}AR/^{39}AR DATA FROM THE TANACROSS D-1 AND D-2, BIG DELTA B-4 AND B-5, AND MOUNT HAYES A-6 QUADRANGLES, ALASKA

Travis J. Naibert, Jeff A. Benowitz, Alicja Wypych, Karri R. Sicard, Evan Twelker

Raw Data File 2018-3

This report has not been reviewed for technical content or for conformity to the editorial standards of DGGS.

$2.00

October 2018
STATE OF ALASKA
DEPARTMENT OF NATURAL RESOURCES
DIVISION OF GEOLOGICAL & GEOPHYSICAL SURVEYS

Reprinted with minor revisions, February 2019.

STATE OF ALASKA
Bill Walker, Governor

DEPARTMENT OF NATURAL RESOURCES
Andrew T. Mack, Commissioner

DIVISION OF GEOLOGICAL & GEOPHYSICAL SURVEYS
Steve Masterman, State Geologist & Director

Publications produced by the Division of Geological & Geophysical Surveys are available to download from the DGGS website (dggs.alaska.gov). Publications on hard-copy or digital media can be examined or purchased in the Fairbanks office:

Alaska Division of Geological & Geophysical Surveys (DGGS)
3354 College Road | Fairbanks, Alaska 99709-3707
Phone: 907.451.5010 | Fax 907.451.5050
dggspubs@alaska.gov | dggs.alaska.gov

DGGS publications are also available at:

Alaska State Library, Historical
Collections & Talking Book Center
395 Whittier Street
Juneau, Alaska 99801

Alaska Resource Library and
Information Services (ARLIS)
3150 C Street, Suite 100
Anchorage, Alaska 99503

Suggested citation:
Naibert, T.J., Benowitz, J.A., Wypych, Alicja, Sicard, K.R., and Twelker, Evan, 2018, 40Ar/39Ar data from the Tanacross D-1 and D-2, Big Delta B-4 and B-5, and Mount Hayes A-6 quadrangles, Alaska: Alaska Division of Geological & Geophysical Surveys Raw Data File 2018-3, 14 p. http://doi.org/10.14509/30112

Reprinted with minor revisions, February 2019.

^{40}AR/^{39}AR DATA FROM THE TANACROSS D-1 AND D-2, BIG DELTA B-4 AND B-5, AND MOUNT HAYES A-6 QUADRANGLES, ALASKA

Travis J. Naibert,[1] Jeff A. Benowitz,[2] Alicja Wypych,[1] Karri R. Sicard,[1] Evan Twelker[1]

INTRODUCTION

This report presents ^{40}Ar/^{39}Ar step-heating geochronology results for igneous and metamorphic rocks from the Alaska Division of Geological & Geophysical Surveys' (DGGS) geologic mapping projects in the Northeastern Tanacross map area in the Tanacross D-1 and D-2 quadrangles, the Richardson map area in the Big Delta B-4 and B-5 quadrangles, and the Wrangellia map area in the Mount Hayes A-6 Quadrangle. Field samples were collected by the DGGS Mineral Resources section during detailed geologic mapping campaigns in 2013 and 2017.

The Northeastern Tanacross map area lies within the Yukon-Tanana terrane on the boundary between the Fortymile and Lake George Assemblages (Dusel-Bacon and others, 2006). The map area encompasses documented porphyry Cu-Mo-Au deposits including Taurus (Harrington, 2010), Fishhook (also known as SW Pika), and Pika Canyon (U.S. Geological Survey, 2008), and is adjacent to the Fortymile Mining District (Yeend, 1996). Previously published geologic mapping includes a reconnaissance 1:250,000-scale map (Foster, 1970) and a slightly modified map published by the USGS (Wilson and others, 2015). New DGGS mapping will provide detailed geologic context for the known porphyry systems in the map area and links to mineral occurrences elsewhere in the region, including across the border in Yukon, Canada.

The Richardson project area in Interior Alaska is approximately 30-50 miles west of the active Pogo gold mine and includes several active intrusion-related gold exploration properties, including Naosi, Uncle Sam, and Democrat Lode. Recent DGGS geologic mapping will improve the understanding of the area's geology and controls on gold mineralization to facilitate industry exploration targeting.

The Wrangellia project area lies along the Denali Highway in the eastern Wrangellia Terrane, which includes magmatic sulfide nickel-copper-cobalt and platinum-group element mineralization hosted in mafic-ultramafic rocks in a structurally complex geologic setting. The sample presented in this report comes from the Clearwater Terrane, described by Jones and others (1987) as an isolated region of metamorphic rock with Permian protoliths (Twelker and O'Sullivan, 2016) caught up in the regional Talkeetna Shear Zone.

DOCUMENTATION OF METHODS

Sample Collection

Fresh, unweathered samples from surface outcrops were collected by DGGS field geologists and were selected for dating based on the presence of sufficiently large crystals and/or fresh aphanitic matrix for whole rock dating. Sample location coordinates (in WGS84 datum) were obtained using GPS-enabled field tablets, with a typical reported accuracy of about 10 meters. Samples were examined under a binocular microscope and in thin section to select unaltered mineral phases before sample preparation.

---

[1] Alaska Division of Geological & Geophysical Surveys, 3354 College Road, Fairbanks, AK 99709; travis.naibert@alaska.gov
[2] University of Alaska Fairbanks Geochronology Laboratory, P.O. Box 755940, Fairbanks, AK 99775-5940

Reprinted with minor revisions, February 2019.

Sample Preparation

For $^{40}Ar/^{39}Ar$ analysis, eight rock samples were submitted to the Geochronology Laboratory at the University of Alaska Fairbanks (UAF). The samples were crushed, sieved, washed, and hand-picked for phenocryst-free rock chips (1,000-500 micron size fraction) and muscovite, biotite, and sericite mineral phases (1000-150 microns). The monitor mineral MMhb-1 (Samson and Alexander, 1987) with an age of 523.5 Ma (Renne and others, 1994) was used to monitor neutron flux (and calculate the irradiation parameter, J). The samples and standards were wrapped in aluminum foil, loaded into aluminum cans of 2.5-cm diameter and 6-cm height. The samples were irradiated in position 5c of the uranium-enriched research reactor at McMaster University in Hamilton, Ontario, Canada for 20 megawatt-hours.

Analytical Methods

Upon their return from the reactor, the samples and monitors were loaded into 2-mm-diameter holes in a copper tray, which was then loaded in an ultra-high-vacuum extraction line. The monitors were fused, and samples heated, using a 6-watt argon-ion laser following the technique described in York and others (1981), Layer and others (1987), and Benowitz and others (2013). Argon purification was achieved using a liquid nitrogen cold trap and a SAES Zr-Al getter at 400°C. The samples were analyzed in a VG-3600 mass spectrometer at the Geophysical Institute, University of Alaska Fairbanks. The argon isotopes measured were corrected for system blank and mass discrimination, as well as calcium, potassium, and chlorine interference reactions following procedures outlined in McDougall and Harrison (1999). Typical full-system 8-minute laser blank values (in moles) were generally 2×10^{-16} mol ^{40}Ar, 3×10^{-18} mol ^{39}Ar, 9×10^{-18} mol ^{38}Ar and 2×10^{-18} mol ^{36}Ar, which are 10–50 times smaller than the sample/standard volume fractions. Correction factors for nucleogenic interferences during irradiation were determined from irradiated CaF_2 and K_2SO_4 as follows: $(^{39}Ar/^{37}Ar)Ca = 7.06 \times 10^{-4}$, $(^{36}Ar/^{37}Ar)Ca = 2.79 \times 10^{-4}$ and $(^{40}Ar/^{39}Ar)K = 0.0297$. Mass discrimination was monitored by running calibrated air shots. The mass discrimination during these experiments was 1.3 percent per mass unit. During sample analysis, calibration measurements were made on a weekly to monthly basis to check for changes in mass discrimination with no significant variation observed during these intervals.

RESULTS AND DISCUSSION

A summary of all the $^{40}Ar/^{39}Ar$ results is provided in the accompanying data tables, with all ages quoted to the ± 1-sigma level and calculated using the constants of Renne and others (2010). The integrated age is the age given by the total gas measured and is equivalent to a potassium-argon (K-Ar) age. Age spectra, Ca/K, and Cl/K plots are included in the appendix. The spectrum provides a plateau age if three or more consecutive gas fractions represent at least 50 percent of the total gas release and are within two standard deviations of each other (Mean Square Weighted Deviation [MSWD] less than 2.5). When a spectrum did not provide a plateau age under the above definition, a weighted-average age was calculated. Below we provide additional discussion of the results of each age analysis, noting our preferred age determination.

17JEA005 – pegmatite, Northeastern Tanacross

A muscovite separate from sample **17JEA005** was analyzed. The integrated age (106.3 ± 0.7 Ma) and the plateau age (105.2 ± 0.7 Ma) are within error. The plateau age **105.2 ± 0.7 Ma** is the preferred age because of the small gas release of the first four step-heat releases. We interpret this age as the age of post-magmatic cooling of the pegmatite dike. No isochron age determination was possible because of the homogenous radiogenic content of the release.

Sample 17JEA005 consists of 55 percent 0.5–6 mm hypidiomorphic feldspar, 35 percent 0.1–3 mm quartz, 7 percent 0.5–4 mm muscovite, 1 percent biotite, and 2 percent <0.5 mm glomeroporphyritic garnet. Pegmatite dike crosscuts foliated biotite gneiss at the sample site. In thin section, feldspars are often twinned and quartz grains have undulatory extinction from deformation. Muscovite is largely unaltered, but flakes are often bent and sometimes twinned in thin section. Similar pegmatite dikes occur throughout the southern part of the Northeastern Tanacross map area; these both crosscut and follow foliation in Lake George Assemblage gneisses and are often observed with aplitic dikes of similar composition. Pegmatite dikes were folded along with the foliation in the metamorphic host rock, indicating that emplacement occurred before deformation ended.

17KS109 – Granite, near Prindle Volcano, Northeastern Tanacross

A biotite separate from sample **17KS109** was analyzed. The step-heat release had a stepping-up age pattern where the higher-temperature steps had older ages than the lower-temperature steps. This pattern is indicative of gas loss/alteration. The analysis did not meet all of the criteria for a plateau age (≥50 percent ^{39}Ar), hence a weighted-average age is presented. The integrated age (99.8 ± 0.8 Ma) and the weighted-average age (110.3 ± 1.8 Ma) are not within error. The weighted average age **110.3 ± 1.8 Ma** is the preferred age because of the documented argon loss. We interpret this age as the age of post-magmatic cooling of the granite. No isochron age determination was possible because of the documented loss.

Sample 17KS109 consists of 50 percent euhedral to subhedral quartz, 45 percent euhedral to subhedral feldspar with fine inclusions of mica, and 5 percent biotite. Grain sizes range from 0.5 to 4 mm. Quartz displays undulatory extinction and cracks in thin section. Sub-grain boundaries overprint feldspar grains. Feldspar is perthitic and twinned. Myrmekite is locally visible. Biotite crystals are finer grained than quartz and feldspar and include minor opaque inclusions; secondary biotite is visible along fractures within feldspar.

17MBW135 – Sericitized felsic dike, Fishhook prospect, Northeastern Tanacross

A sericite separate from sample **17MBW135** was analyzed. The integrated age (63.8 ± 0.4 Ma) and the plateau age (63.7 ± 0.5 Ma) are within error. The plateau age **63.7 ± 0.5 Ma** is the preferred age because of the high atmospheric content of the first four step-heat releases. We interpret this age to be the age of alteration at the Fishhook prospect. No isochron age determination was possible because of the homogenous radiogenic content of the release.

Sample 17MBW135 consists of 7 percent euhedral to subhedral, partially altered biotite, 5 percent quartz up to 3 mm, 3 percent sericite <2 mm, and 90 percent groundmass, which consists mostly of fine-grained sericite and quartz.

17MBW213 – Diorite, Pika area, Northeastern Tanacross

A biotite separate from sample **17MBW213** was analyzed. The integrated age (65.4 ± 0.5 Ma) and the plateau age (66.3 ± 0.6 Ma) are within error. The plateau age **66.3 ± 0.7 Ma** is the preferred age because of the high atmospheric content of the first four step-heat releases. We interpret this age as the age of post-magmatic cooling of the diorite. No isochron age determination was possible because of the homogenous radiogenic content of the release.

Sample 17MBW213 consists of 60 percent 0.5–5 mm euhedral to subhedral feldspar phenocrysts, 20 percent <0.5 mm anhedral quartz, 15 percent subhedral biotite, 5 percent <1 mm subhedral hornblende, and <1 percent opaque minerals as inclusions in feldspar, biotite, and hornblende. Feldspar phenocrysts are compositionally zoned and have polysynthetic twinning. Biotite is medium-grained, tabular flakes with minor chlorite overgrowths and opaque inclusions. Hornblende is mostly altered to chlorite.

17MBW228 – Altered dacite, Pika area, Northeastern Tanacross

A whole rock separate from sample **17MBW228** was analyzed. The integrated age (64.3 ± 0.4 Ma) and the plateau age (65.5 ± 0.4 Ma) are within error. The plateau age **65.5 ± 0.4 Ma** is the preferred age because of the high atmospheric-argon content of the first four step-heat releases. We interpret this age as the age of post-magmatic cooling of the dacite. No isochron age determination was possible because of the homogenous radiogenic content of the release.

Sample 17MBW228 consists of 12 percent <2 mm feldspars, which are partly resorbed, 6 percent hornblende with many inclusions, <2 percent opaque minerals (likely magnetite), and 80 percent groundmass, dominantly consisting of quartz and feldspar. The sample appears to be a dacite flow above a hydrothermal breccia related to the underlying Pika plutonic system. Feldspar phenocrysts are twinned, partly altered to clays, and include abundant opaque inclusions. Hornblende is altered to chlorite.

17ET192 – muscovite-bearing granite, Naosi prospect, Richardson

A muscovite separate from sample **17ET192** was analyzed. The integrated age (101.9 ± 0.7 Ma) and the plateau age (100.0 ± 0.7 Ma) are within error. The plateau age **100.0 ± 0.7 Ma** is the preferred age because of the low gas release of the first four step-heat releases. We interpret this age to reflect post-magmatic cooling of the granite. No isochron age determination was possible because of the homogenous radiogenic content of the release.

Sample 17ET192 consists of 40 percent subhedral to anhedral quartz, 50 percent potassium feldspar, 7 percent muscovite, 3 percent biotite, which has mostly been altered to chlorite, and <1 percent tourmaline and garnet, which were observed in outcrop but not in thin section. The sample is fine grained (<1 mm). Quartz has undulose extinction and irregular crystal edges, potassium feldspar is perthitic. Muscovite, a primary phase, is rarely twinned; it also occurs as abundant inclusions within feldspar grains.

17MBW331 – biotite-bearing granite, Richardson

A biotite separate from sample **17MBW331** was analyzed. The integrated age (102.8 ± 0.7 Ma) and the plateau age (103.5 ± 0.7 Ma) are within error. The plateau age **103.5 ± 0.7 Ma** is the preferred age because of the high atmospheric content of the first step-heat release. We interpret this age to reflect post-magmatic cooling of the granite. No isochron age determination was possible because of the homogenous radiogenic content of the release.

Reprinted with minor revisions, February 2019.

Sample 17MBW331 consists of 25 percent anhedral <1.5 mm quartz, 60 percent euhedral to subhedral feldspar up to 15 mm, 15 percent fresh, undeformed biotite with very minor chlorite alteration, and <1 percent garnet up to 0.5 mm. Potassium feldspar displays lamellar twins and inclusions of biotite. Granophyric textures of quartz and potassium feldspar are present in some areas, Quartz has weak undulose extinction and often occurs as inclusions within feldspar grains. Minor sericite is replacing feldspar. Biotite also occurs in masses along feldspar and quartz boundaries.

13ET295 – felsic schist (metavolcanic), Wrangellia

A muscovite separate from sample **13ET295** was analyzed. The step-heat release had a stepping-up age pattern where the higher temperature steps had older ages than the lower temperature steps. This pattern is indicative of gas loss/alteration. The analysis did not meet all of the criteria for a plateau age ($\geq$50 percent ^{39}Ar), hence a weighted-average age is presented. The integrated age (103.4 ± 0.6 Ma) and the weighted-average age (112.6 ± 0.7 Ma) are not within error. The weighted average age **112.6 ± 0.7 Ma** is the preferred age because of the documented argon loss. We interpret this age to reflect metamorphic cooling of the schist, with lower-temperature steps indicating argon loss during a younger partial resetting event. No isochron age determination was possible because of the documented loss.

Sample 13ET295 is a metavolcanic felsic schist consisting of 3 percent subhedral feldspar (0.5 mm), and 1 percent quartz (0.5 mm) porphyroclasts in fine-grained granoblastic quartz groundmass (75 percent) with white mica partings (15 percent) and minor carbonate (5 percent) and opaque minerals (1 percent).

ACKNOWLEDGMENTS

The DGGS 2017 Northeastern Tanacross and Richardson projects were funded through State of Alaska general funds. The Wrangellia project was funded by Capital Improvement Project funds through the State's Strategic and Critical Minerals Assessment project. The authors acknowledge the contributions of the 2017 Richardson and Northeastern Tanacross project field crew: Melanie B. Werdon, Jen E. Athey, Amanda L. Willingham, Alec C. Lockett, and the 2013 Wrangellia field crew: Larry K. Freeman, Rainer J. Newberry, Erik N. Bachmann, David A. Reioux, Amy L. Tuzzolino, and T. Colby Wright.

Reprinted with minor revisions, February 2019.

REFERENCES

Benowitz, J.A., Layer, P.W., and VanLaningham, Sam., 2013, Persistent Long-Term (~24 Ma) Exhumation in the Eastern Alaska Range Constrained by Stacked Thermochronology, Geological Society of London Special Publication 378, p. 225–243.

Dusel-Bacon, Cynthia., Hopkins, M.J., Mortensen, J.K., Dashevsky, S.S., Bressler, J.R., and Day, W.C., 2006, Paleozoic tectonic and metallogenic evolution of the pericratonic rocks of east-central Alaska and adjacent Yukon, *in* Colpron, Maurice, and Nelson, J.L. eds., Paleozoic Evolution and Metallogeny of Pericratonic Terranes at the Ancient Pacific Margin of North America, Canadian and Alaskan Cordillera: Geological Association of Canada, Special Paper 45, p. 25–74.

Foster, H.L., 1970, Reconnaissance Geologic Map of the Tanacross Quadrangle, Alaska: U.S. Geological Survey Miscellaneous Geologic Investigations Map 593, 1 sheet, scale 1:250,000.

Harrington, Edward, 2010, Taurus Property: Technical Report for Senator Minerals INC, 133 p. (posted on www.sedar.com).

Jones, D.L., Silberling, N.J., Coney, P.J., and Plafker, George, 1987, Lithotectonic terrane map of Alaska (west of the 141st meridian): U.S. Geological Survey Miscellaneous Field Studies Map 1874-A, 1 sheet, scale 1:2,500,000.

Layer, P.W., Hall, C.M. and York, Derek., 1987, The derivation of $^{40}Ar/^{39}Ar$ age spectra of single grains of hornblende and biotite by laser step heating: Geophysical Research Letters, v. 14, p. 757–760.

McDougall, Ian and Harrison, T.M., 1999, Geochronology and Thermochronology by the $^{40}Ar/^{39}Ar$ method-2nd edition, Oxford University Press, New York, 269 p.

Renne, P.R., Mundil, Roland, Balco, Greg, Min, Kyoungwon, and Ludwig, K.R., 2010, Joint determination of ^{40}K decay constants and 40Ar*/40K for the Fish Canyon sanidine standard, and improved accuracy for $^{40}Ar/^{39}Ar$ geochronology: Geochimica et Cosmochimica Acta, v. 74, n. 18, p. 5349–5367.

Renne, P.R., Deino, A.L., Walter, R.C., Turrin, B.D., Swisher, C.C., Becker, T.A., Curtis, G.H., Sharp. W.D., and Jaouni, A.R., 1994, Intercalibration of astronomical and radioisotopic time: Geology, v. 22, n. 9, p. 783–786.

Samson, S.D., and Alexander, E.C., 1987, Calibration of the interlaboratory $^{40}Ar/^{39}Ar$ dating standard, MMhb1. Chemical Geology, v. 66, p. 27–34.

Twelker, Evan, and O'Sullivan, P.B., 2016, U-Pb zircon age data from meta-igneous rocks in the Clearwater Mountains, Mount Hayes A-6 Quadrangle, Alaska: Alaska Division of Geological & Geophysical Surveys Raw Data File 2016-8, 17 p. http://doi.org/10.14509/29663

U.S. Geological Survey, 2008, Alaska resource data file, new and revised records version 1.7, Open-File Report 2008-1225, p. 2144–2149.

Yeend, Warren, 1996, Gold placers of the historical Fortymile River region, Alaska: U.S. Geological Survey Bulletin 2125, 75 p., 1 sheet, scale 1:63,360.

York, Derek., Hall, C.M., Yanase, Yotaro, Hanes, J.A., and Kenyon, W.J., 1981, $^{40}Ar/^{39}Ar$ dating of terrestrial minerals with a continuous laser: Geophysical Research Letters, v. 8, p. 1136–1138.

Wilson, F.H., Hults, C.P., Mull, C.G., and Karl, S.M., 2015, Geologic map of Alaska: U.S. Geological Survey Scientific Investigations Map 3340, 197 p., 2 sheets, scale 1:1,584,000.

Reprinted with minor revisions, February 2019.

APPENDIX: PLOTS OF ^{40}AR/^{39}AR AGE SPECTRA AND CA/K AND CL/K RATIOS

17JEA005

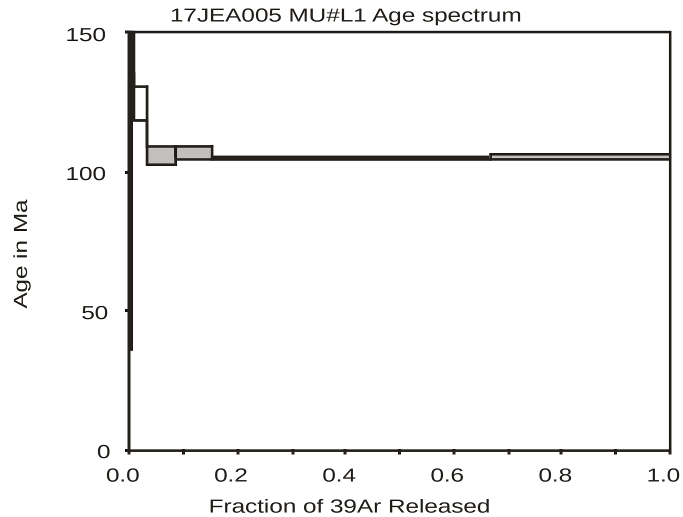

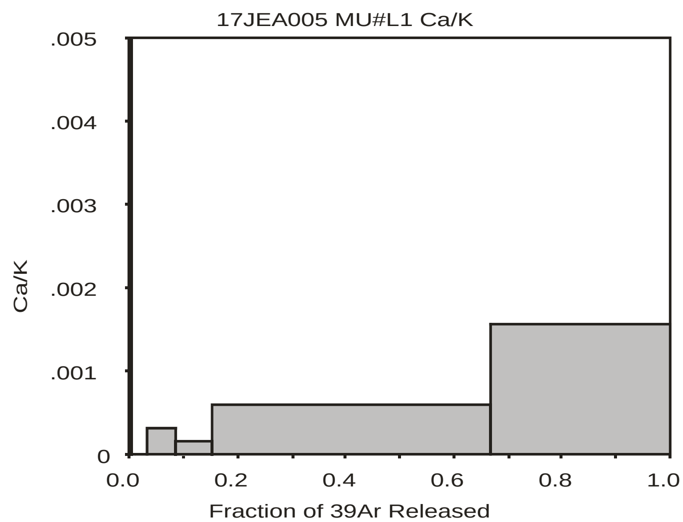

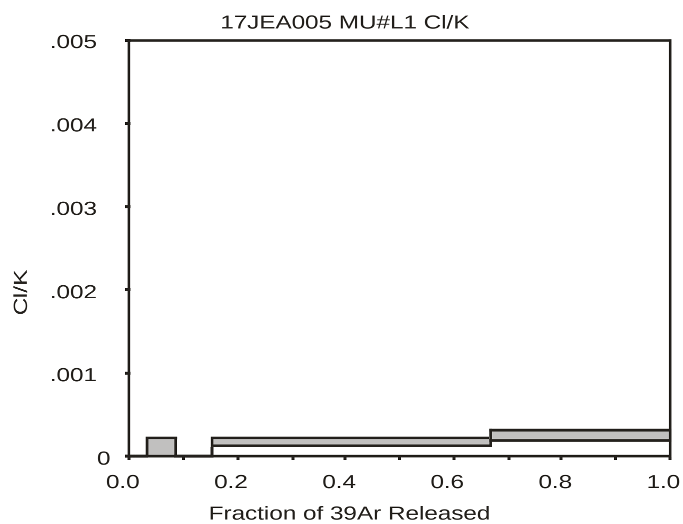

Reprinted with minor revisions, February 2019.

17KS109

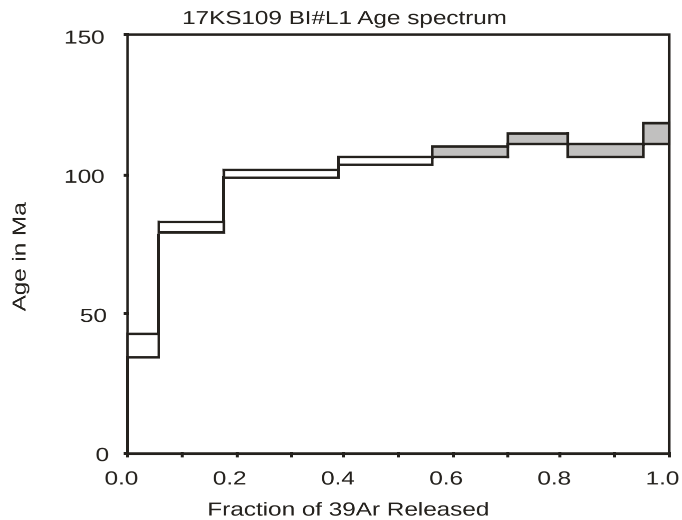

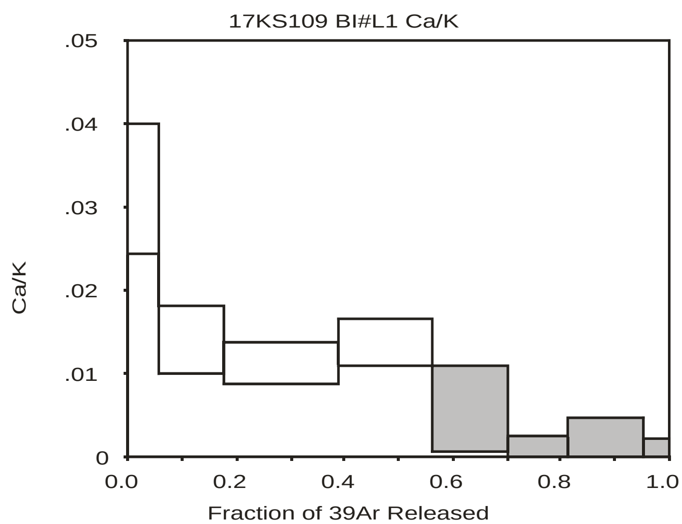

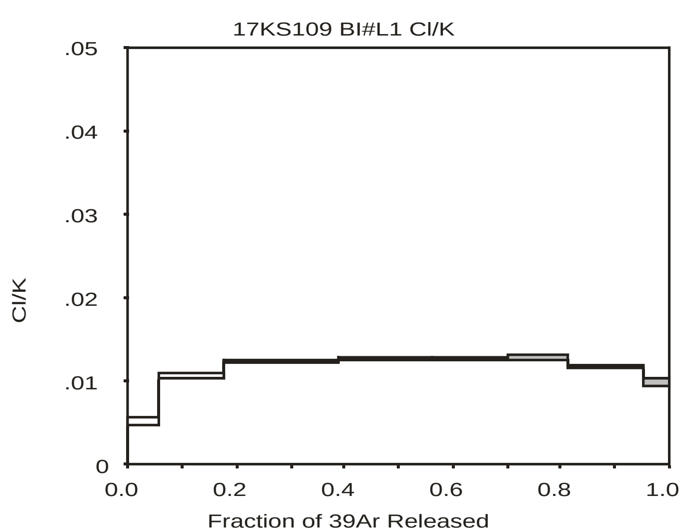

Reprinted with minor revisions, February 2019.

17MBW135

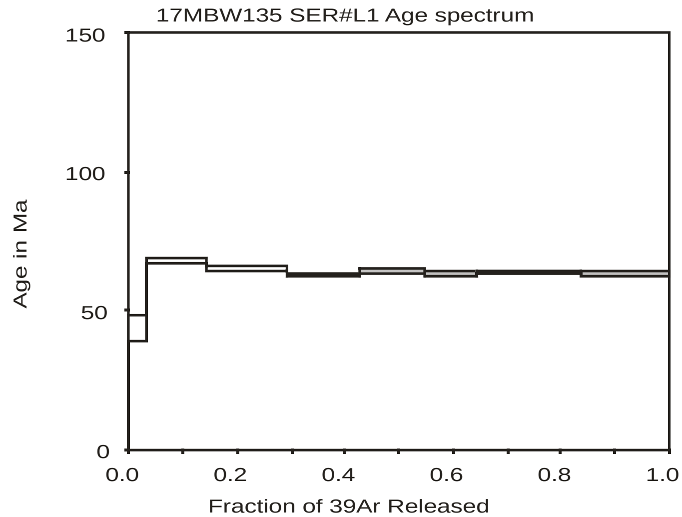

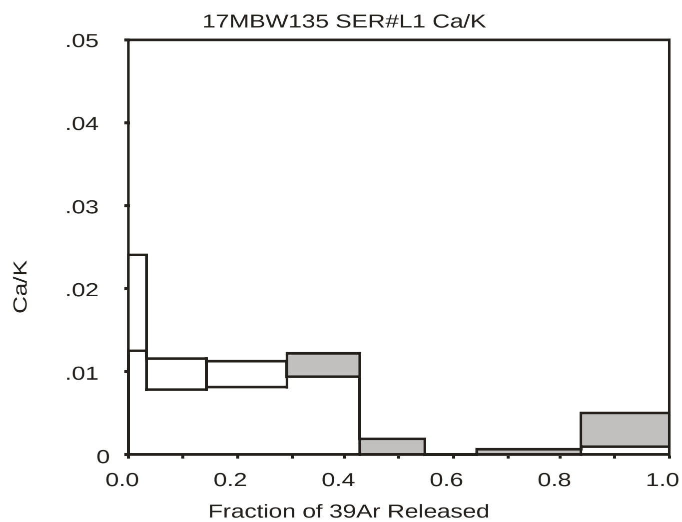

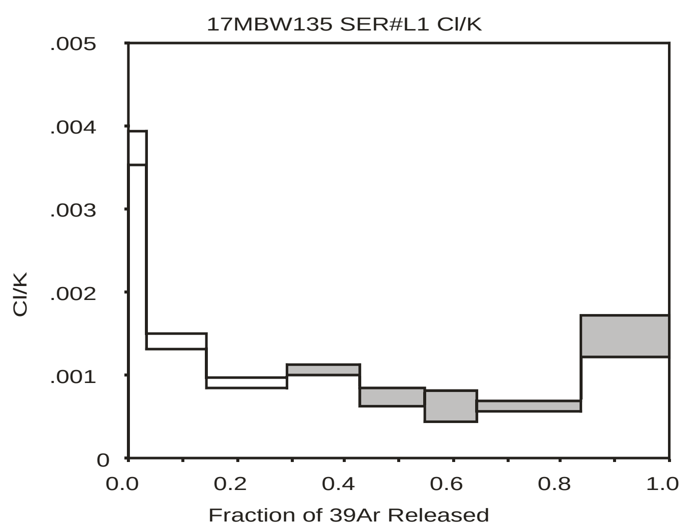

Reprinted with minor revisions, February 2019.

17MBW213

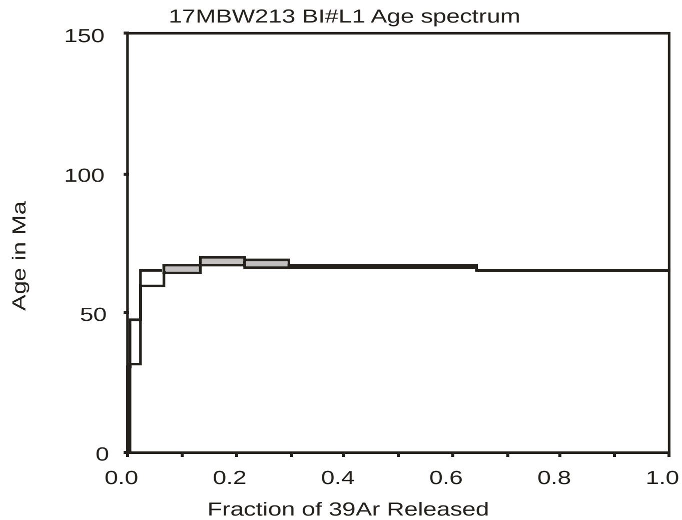

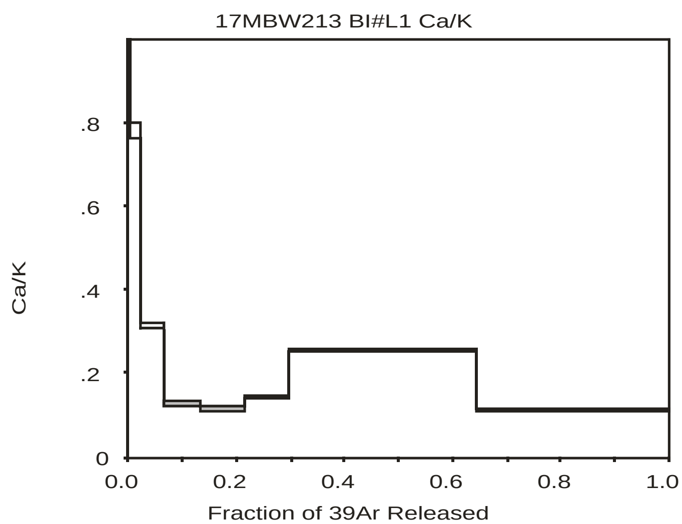

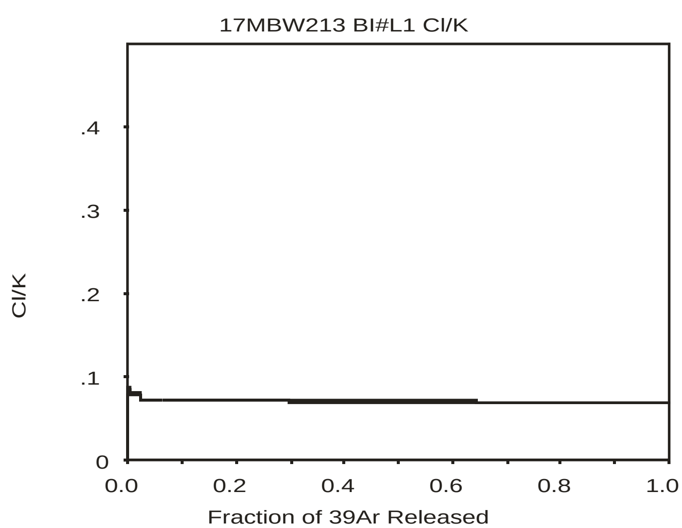

Reprinted with minor revisions, February 2019.

17MBW228

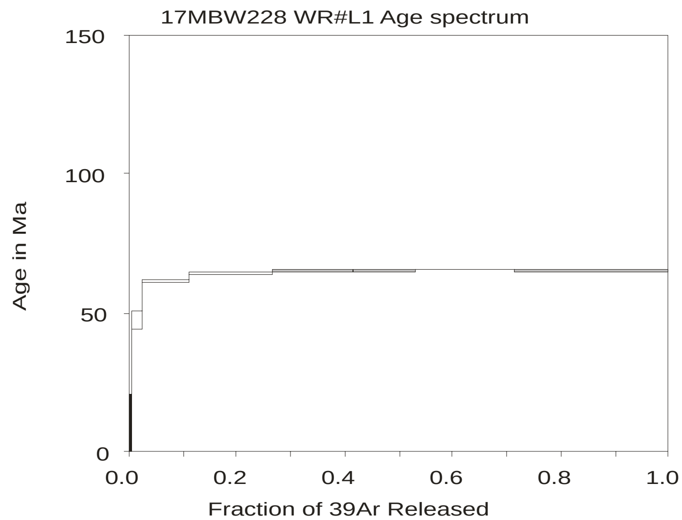

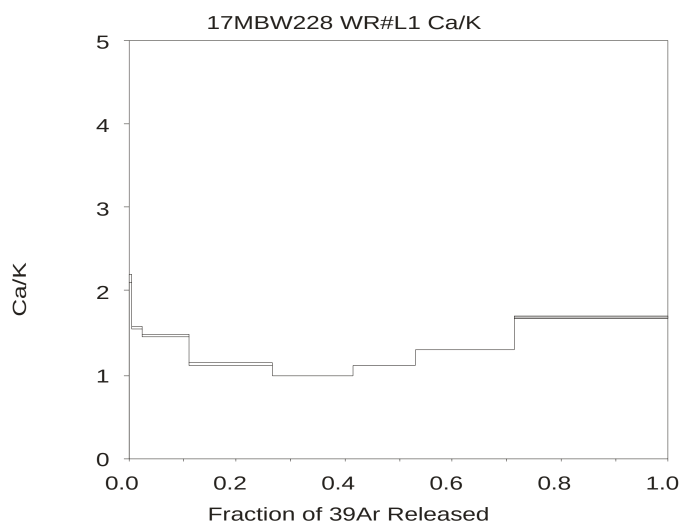

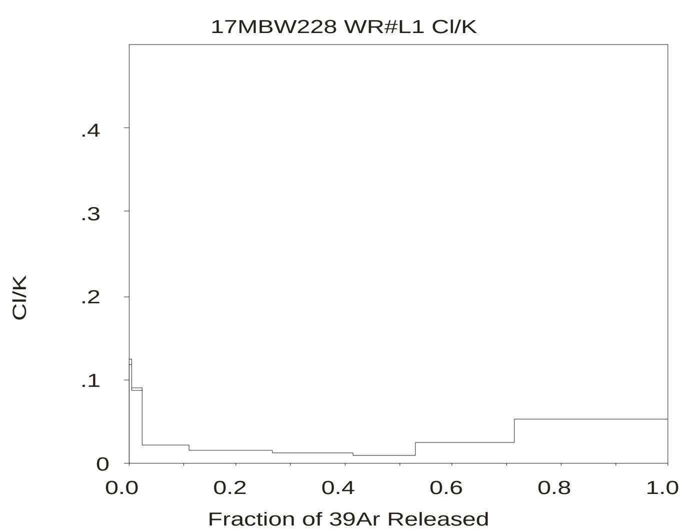

Reprinted with minor revisions, February 2019.

17ET192

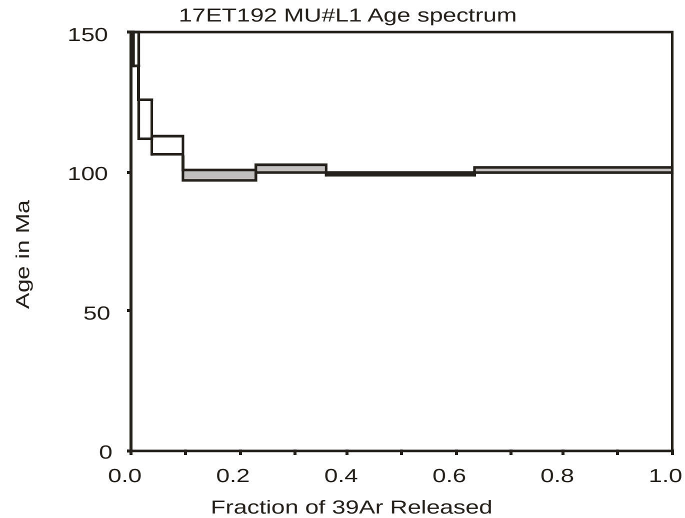

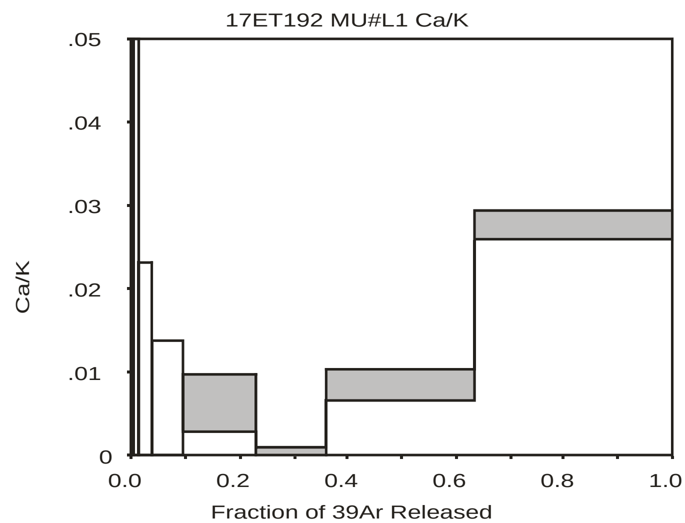

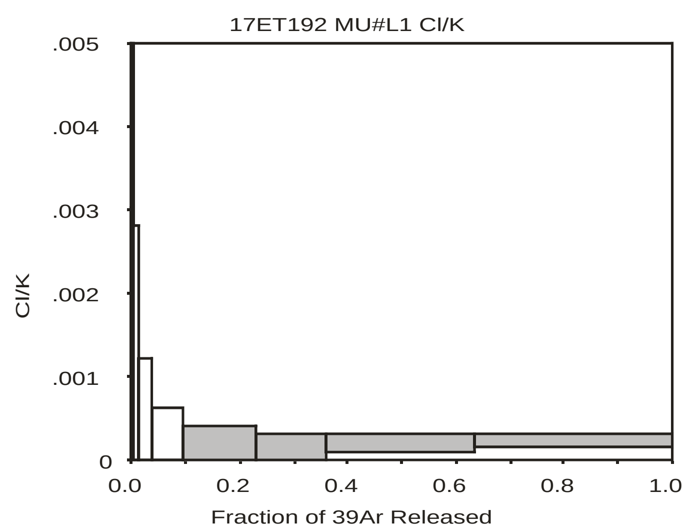

Reprinted with minor revisions, February 2019.

17MBW331

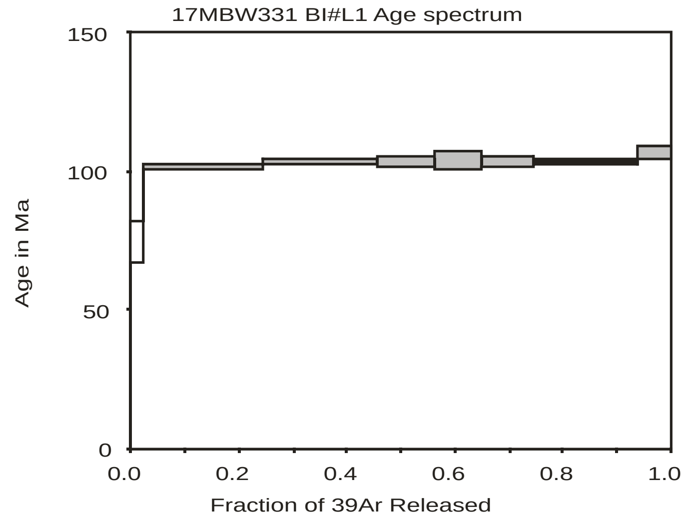

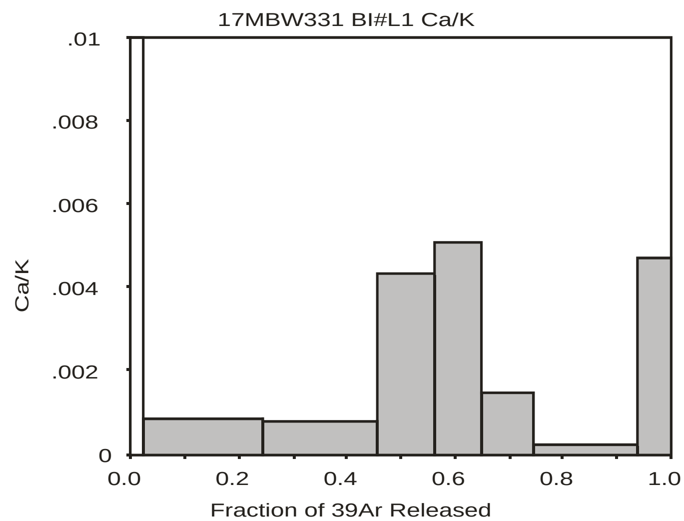

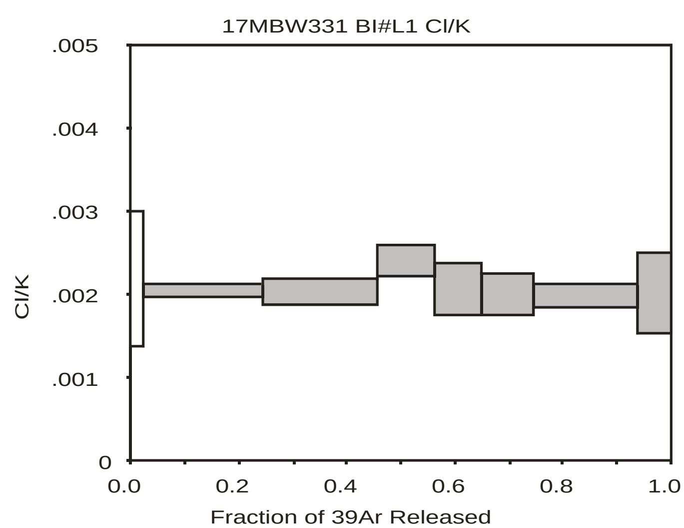

Reprinted with minor revisions, February 2019.

13ET295

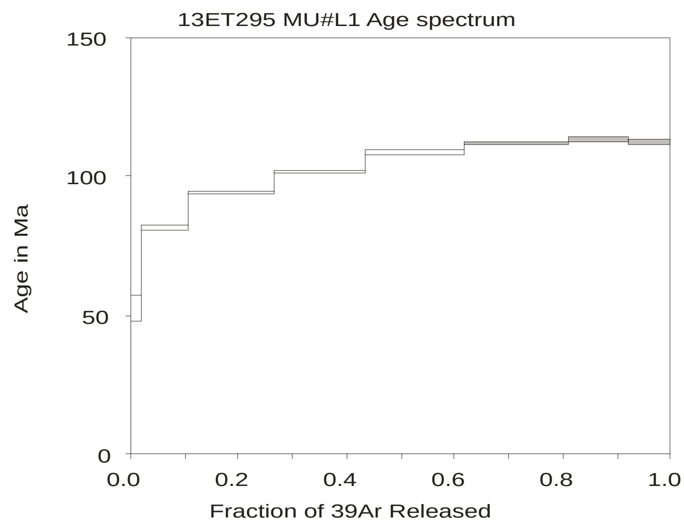

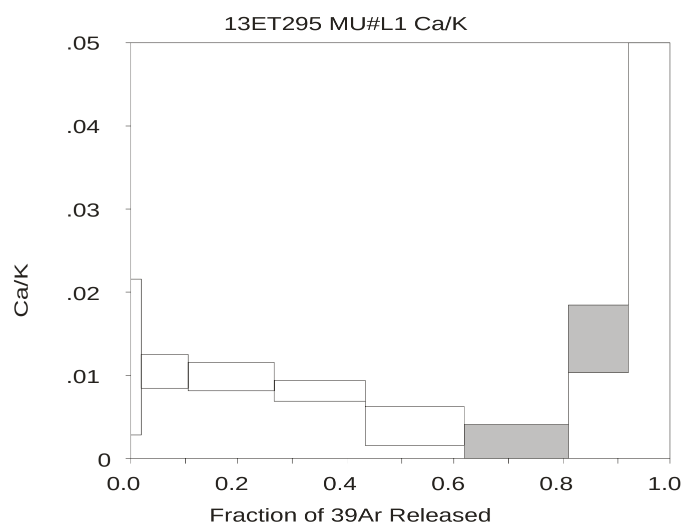

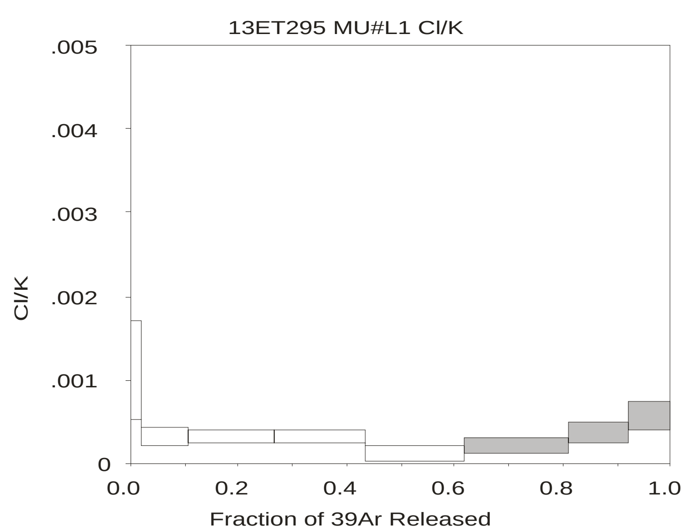

Reprinted with minor revisions, February 2019.